PHYSICS

Automatic exposure control in CT: the effect of patient size, anatomical region and prescribed modulation strength on tube current and image quality

Antonios E. Papadakis · Kostas Perisinakis · John Damilakis

Abstract

Objectives To study the effect of patient size, body region and modulation strength on tube current and image quality on CT examinations that use automatic tube current modulation (ATCM).

Methods Ten physical anthropomorphic phantoms that simulate an individual as neonate, 1-, 5-, 10-year-old and adult at various body habitus were employed. CT acquisition of head, neck, thorax and abdomen/pelvis was performed with ATCM activated at weak, average and strong modulation strength. The mean modulated mAs (mAs_{mod}) values were recorded. Image noise was measured at selected anatomical sites.

Results The mAs_{mod} recorded for neonate compared to 10-year-old increased by 30 %, 14 %, 6 % and 53 % for head, neck, thorax and abdomen/pelvis, respectively, ($P<0.05$). The mAs_{mod} was lower than the preselected mAs with the exception of the 10-year-old phantom. In paediatric and adult phantoms, the mAs_{mod} ranged from 44 and 53 for weak to 117 and 93 for strong modulation strength, respectively. At the same exposure parameters image noise increased with body size ($P<0.05$).

Conclusions The ATCM system studied here may affect dose differently for different patient habitus. Dose may decrease for overweight adults but increase for children older than 5 years old. Care should be taken when implementing ATCM protocols to ensure that image quality is maintained.

A. E. Papadakis (✉)
Department of Medical Physics, University Hospital of Heraklion, Stavrakia, P.O. Box 1352, Heraklion 71110, Crete, Greece
e-mail: apapadak@edu.med.uoc.gr

K. Perisinakis · J. Damilakis
Faculty of Medicine, Department of Medical Physics, University of Crete, P.O. Box 2208, Heraklion 71003, Crete, Greece

Key Points
- *ATCM efficiency is related to the size of the patient's body.*
- *ATCM should be activated without caution in overweight adult individuals.*
- *ATCM may increase radiation dose in children older than 5 years old.*
- *ATCM efficiency depends on the protocol selected for a specific anatomical region.*
- *Modulation strength may be appropriately tuned to enhance ATCM efficiency.*

Abbreviations

ATCM	Automatic tube current modulation
CIR	Circumference
CT	Computed tomography
HU	Hounsfield unit
mAs_{mod}	Mean modulated mAs
ROI	Region of interest
SD	Standard deviation
ROI	Region of interest

Introduction

Automatic tube current modulation (ATCM) systems adapt the tube current on the basis of each patient's attenuation characteristics and aim to generate images of diagnostic quality at the lowest possible radiation dose. Previous studies have reported that ATCM systems can reduce patient radiation dose by up to 60 % compared to the fixed tube current examinations [1–5]. However, the degree of radiation dose reduction is strongly influenced by the patient's size and the anatomy of

the imaged body volume. The pattern of tube current modulation is determined by a certain image quality metric, which is different between ATCM schemes. This image quality metric is specified in the form of either image noise or a reference mAs value [6–8]. The level of this metric is selected by the user on the patient size and anatomic region being examined, while in paediatric patients it is selected also depending on the age of the examined individual.

The ATCM system implemented by Siemens Medical Solutions (CARE Dose 4D, Siemens, Erlangen, Germany) adapts the tube current through two parameters recommended for each different body region, but is still operator-defined in terms of (i) the quality reference milliampere-second value (mAs_{QR}), and (ii) the modulation strength setting i.e. weak, average or strong [9, 10]. To achieve exposure optimization, operators must tailor the mAs_{QR} and modulation strength for each region to be examined and patient size. This, however, requires an astute understanding of how the above parameters influence resulting image quality and patient radiation dose. Despite the fact that several studies have been published on the dose reduction from ATCM systems, there is no published data on the effect of patient size and modulation strength on tube current and image quality [11, 12]. Thus, the effectiveness of ATCM during examinations performed on overweight patients is not known. Moreover, the impact of altering the ATCM modulation strength setting on radiation dose and image quality in patients of varying size is not known.

The aim of the present study was to examine systematically the effect of patient size, patient anatomy and prescribed modulation strength on tube current and image quality in CT examinations that use ATCM.

Materials and methods

Anthropomorphic phantoms

Four physical anthropomorphic phantoms (ATOM Phantoms, CIRS, Norfolk, Virginia, USA) that represent the average individual as neonate, 1-year-old, 5-year-old, 10-year-old child and the Rando phantom (Alderson Research Labs, Stanford, CA, USA) that simulates the average adult individual were employed. A whole body lateral scout view of each phantom is shown in Fig. 1.

To simulate patients with increased body size, the phantoms were appropriately modified into different body habitus using bolus material. Bolus is made of a homogeneous, tissue-equivalent gel with a density 1.03 g/cm^3 (CIVCO Medical Solutions, Iowa, USA). The bolus material is formed in rectangular sheets, 35 cm×35 cm, and can be cut to any shape with scissors. The thickness of the bolus sheet was 2 cm.

One bolus (Fig. 1e) and two bolus sheets (Fig. 1f) were placed around the anterior surface of the abdomen and pelvis

slabs of the 10-year-old phantom. The aforementioned bolus sheets were cut into 30 cm×30 cm squares and covered the phantom slabs numbered from 19 to 31. These phantom configurations allow the simulation of a 10-year-old child at three different body sizes, i.e. normal weight and overweight at two different habitus. The 10-year-old phantom in the last two body habitus is designated hereafter as 10-year-old (I) and 10-year-old (II). One bolus sheet 2 cm thick (Fig. 1h) was placed around the anterior surface of the abdomen and pelvis slabs of the adult phantom. This bolus sheet was 35 cm× 35 cm and covered the phantom slabs numbered from 15 to 32. The phantom configured in this body habitus is designated hereafter as adult (I). Two bolus sheets were additionally added, resulting in a total bolus thickness of 6 cm (Fig. 1i). These bolus sheets covered the adult phantom slabs numbered from 17 to 31. The phantom configured in this body habitus is designated hereafter as adult (II). Finally, two additional bolus sheets were added around the anterior surface of the abdomen and pelvis slabs of the adult phantom (Fig. 1j), resulting in a total bolus thickness of 10 cm. The inferior bolus sheet covered the phantom slabs numbered from 22 to 29, while the superior bolus sheet covered the phantom slabs numbered from 20 to 30. The phantom configured in this body habitus is designated hereafter as adult (III). The above phantom configurations allow the simulation of an adult individual at four different body sizes, i.e. normal weight, and overweight at three different body habitus (I), (II) and (III). Thus, these phantoms exhibit a progressively increasing attenuation of the x-ray beam in the abdominal and pelvic regions.

Weight and height values of each phantom are listed in Table 1. To obtain an index of the body size of each phantom, circumference measurements were performed in specific anatomical sites of each body region. Head circumference was measured at the axial image depicting the maxillary sinuses. Neck circumference was measured at the axial image depicting the fourth cervical vertebrae. Thorax circumference was measured at the axial image depicting the central lung parenchyma. Abdomen circumference was measured at the axial CT image depicting the superior part of the iliac crest.

CT system and ATCM mechanism

A 16-slice CT system (Sensation 16, Siemens, Germany) equipped with the CARE Dose 4D (software version syngo CT 2006G, Siemens, Germany) ATCM system was used. ATCM is accomplished by modulating the tube current both angularly and along the z-axis of the patient according to each patient's individual anatomy [9–14]. The tube current is modulated according to the difference in the recorded attenuation between the examined individual and an average sized patient, named as the 'reference patient'. An image quality reference mAs (mAs_{QR}) setting is preselected for the reference patient according to the diagnostic requirements. On the basis of the
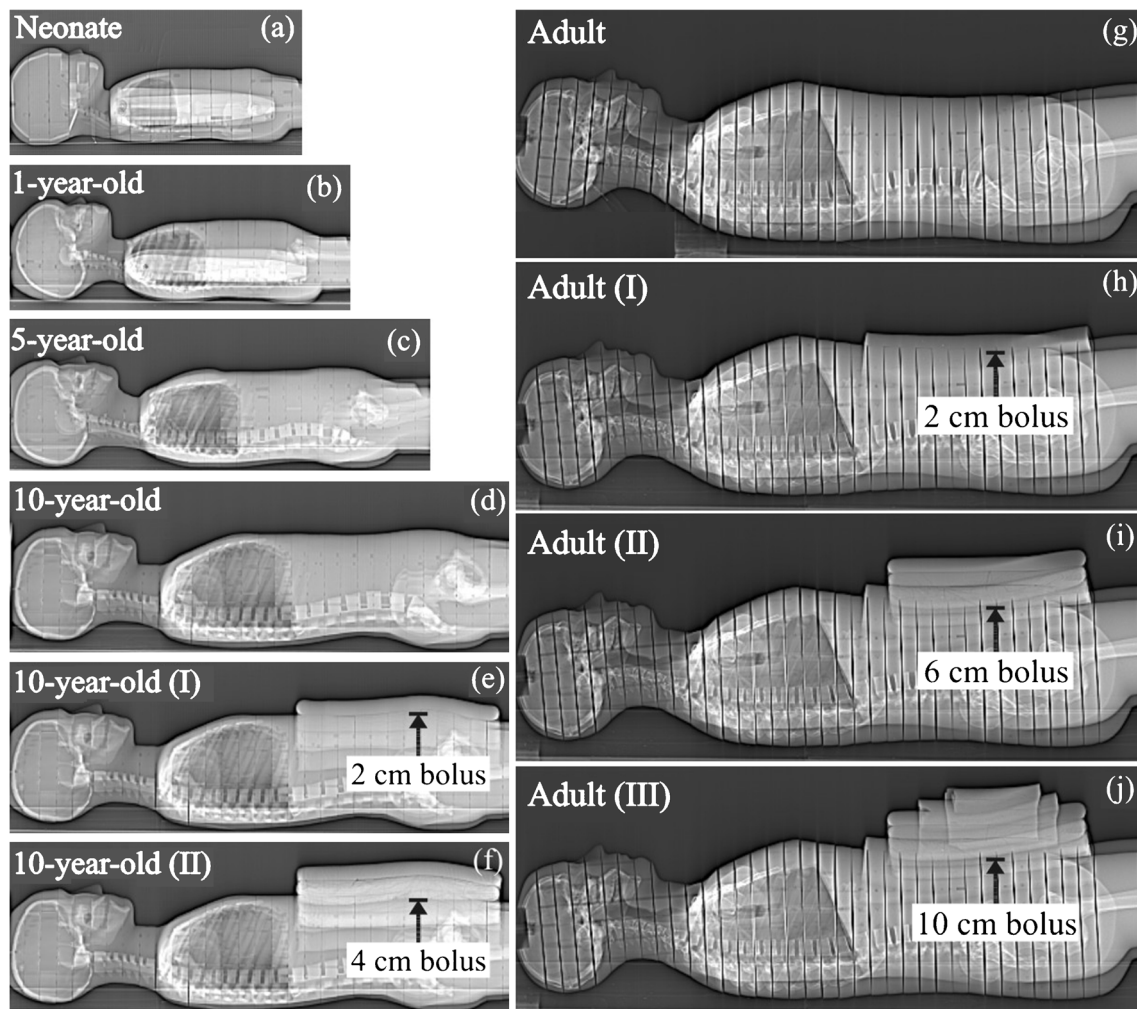
Fig. 1 A lateral scout view of the anthropomorphic phantoms employed. The torso of the 10-year-old and adult phantoms was modified using sheets of bolus material to increase x-ray beam attenuation in the abdomen and pelvis anatomical region

topogram, the system determines whether the patient's body size is smaller or larger compared to the reference patient. If the algorithm detects that the examined body part is smaller than the reference patient's, the system prescribes a decrease

Table 1 Weight and height values of each phantom

Age	Weight (kg)	Height (cm)
Neonate	3.5	51
1-year-old	10	75
5-year-old	19	110
10-year-old	32	140
10-year-old (I)	NA	140
10-year-old (II)	NA	140
Adult	73.5	173
Adult (I)	NA	173
Adult (II)	NA	173
Adult (III)	NA	173

NA not available

in tube current below mAs_{QR}. Similarly, if the algorithm detects that the examined body part is larger compared to the reference patient, the system prescribes an increase in tube current above mAs_{QR}. Hence, when imaging smaller or larger patients compared to the reference patient, images of lower or higher noise levels, respectively, are generated. According to the manufacturer, the reference patient for adult examinations is defined as a typical adult weighing 70 kg. For child examinations, the reference patient is defined as a typical 5-year-old child weighing 20 kg. In the current study, the Rando phantom was considered as the reference patient for the adult examinations and the ATOM phantom simulating the average 5-year-old individual was considered as the reference patient for the paediatric examinations. The ATCM system allows the selection of the modulation strength on the basis of the anatomical characteristics of the examined patient. Prior to the acquisition of the scout view, the operator is allowed to choose the required modulation strength, which will be applied in the examination. Three modulation strength options (weak, average and strong decrease) are available for slim or undersized

anatomical regions compared to the reference patient. Additionally, three modulation strength options (weak, average and strong increase) are available for obese or oversized anatomical regions compared to the reference patient. Any of the three modulation strength options for slim anatomical regions may be combined with any of the three modulation strength options for obese anatomical regions, resulting in nine different combinations. Figure 2 demonstrates the theoretical effect of the CARE Dose4D system on tube current and image noise [9]. For the slim, strong decrease setting, the tube current is decreased less than constant noise would require. For the obese, strong increase setting, the tube current is increased less than constant noise would require.

CT imaging protocols

To assess the effect of the ATCM in different anatomical regions on tube current and image noise, head, neck, thorax and abdomen/pelvis CT acquisitions were performed using the routine examination protocols specified for children (Table 2). These CT acquisitions were also performed using the routine examination protocols specified for adults (Table 3) to assess the effect of patient target group on tube

current and image noise. Figure 3 illustrates the imaging boundaries of each anatomical region on an AP scout view of the 10-year-old phantom. Each phantom was examined using the quality reference mAs (mAs_{QR}) setting, which is prescribed by the routine examination protocol for a particular anatomical region (Tables 2 and 3). The mean modulated mAs_{mod} value displayed in the system console was recorded upon the end of each helical image.

To compare modulated tube current among different examination protocols applied at the same anatomical region, whole body CT examinations were performed in 5-year-old and adult phantoms using all anatomic-specific routine examination protocols listed in Tables 2 and 3. To facilitate comparison on modulated tube current among protocols, all whole body CT examinations were performed at the same mAs_{QR} setting. Upon the completion of each ATCM-activated whole body acquisition, the modulated tube current–time product (mAs_{mod}) value was manually recorded from the DICOM header of each consecutive reconstructed axial image along the z-axis. These values were used to generate plots of $mAs_{mod}(z)$ profiles.

All CT acquisitions were performed with the ATCM modulation strength set to (i) 'strong decrease'–'weak increase', (ii) 'average decrease'–'average increase' and (iii) 'weak
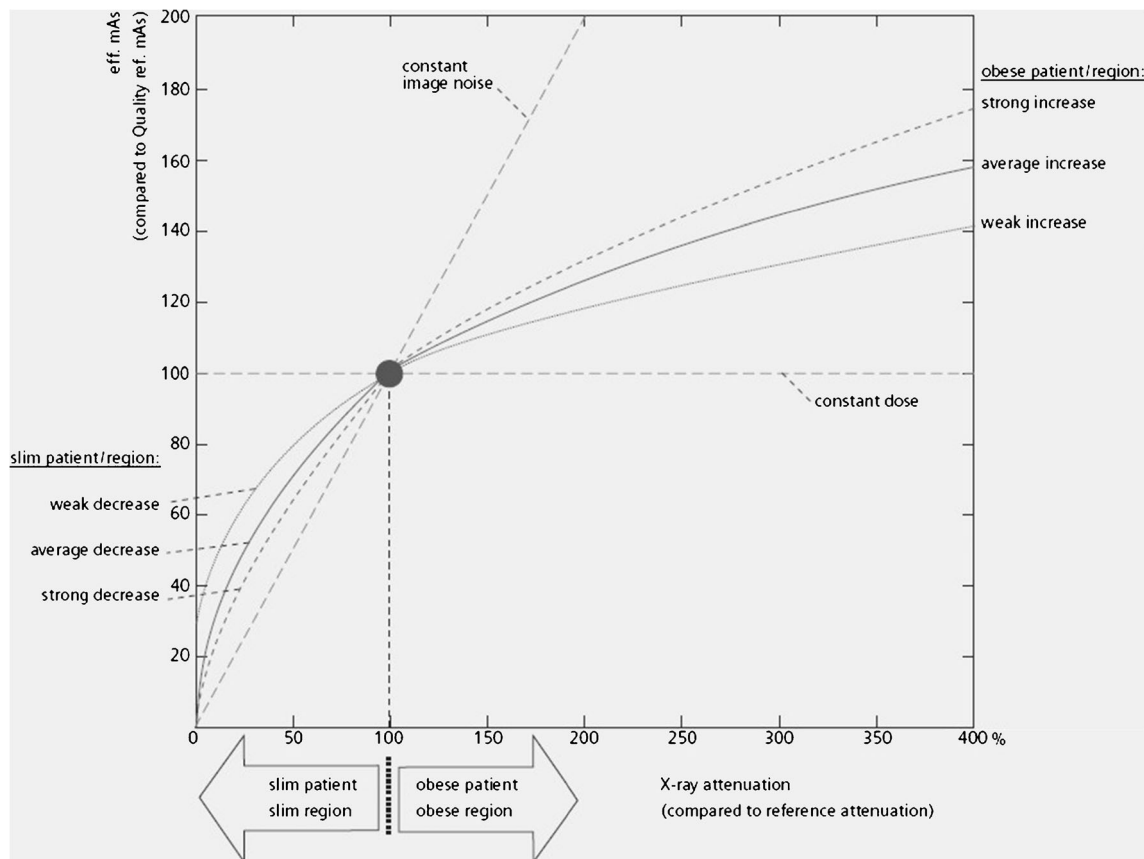

Fig. 2 CARE Dose 4D: a theoretical illustration of the weak (*dotted curve*), average (*solid curve*) and strong (*dashed curve*) modulation strength effect on tube current versus x-ray attenuation in relation to constant image noise (*dashed diagonal line*)

Table 2 Routine 'child' examination protocols

Anatomical region	Protocol acquisition parameters for routine CT examinations specified for children			
	Head	Neck	Thorax	Abdomen & pelvis
Examination protocol	Head routine	Neck routine	Thorax routine	Abdomen routine
Parameter				
kV	120	120	120	120
Quality reference mAs	150	60	30	55
Beam width (mm)	16×1.5	16×1.5	16×1.5	16×1.5
Pitch	0.55	0.75	1.15	1.15
Rotation time (s)	0.75	0.75	0.5	0.5
Reconstruction kernel	C30s	B30s	B30f	B30f

The protocol acquisition parameters for each anatomical region in routine CT examination protocols specified for children

decrease'–'strong increase'. These settings were selected because they correspond to the lowest, the average and the highest patient exposure, respectively. The 'average decrease'/'average increase' is the default modulation strength set by the manufacturer. All phantoms were accurately aligned with the gantry isocentre, while in the supine position. Each phantom and table increment was kept stable among acquisitions. All ATCM-activated acquisitions were repeated five times to calculate arithmetic averages of the modulated tube current–time product values among images.

To investigate whether the ATCM-activated acquisitions can deliver images of similar noise at reduced radiation dose compared to acquisitions performed with the ATCM system deactivated, the phantoms were subjected to head, neck, thorax and abdomen/pelvis examinations using the routine examination protocols (Tables 1 and 2) at fixed tube current settings (mAs_f). The mAs_f settings applied were based on the guidelines proposed by the system's application guide on phantom's age for head and neck, and phantom's weight for torso examinations [10]

Quantitative image noise assessment and statistical analysis

To quantitatively assess the effect of ATCM on image quality, image noise was measured as the average standard deviation (SD) of the Hounsfield unit (HU) values across circular 2 cm^2 regions of interest (ROI), which were drawn over uniform, tissue-equivalent areas. For head anatomical region, image noise was measured in brain equivalent areas at the level of the central part of the brain parenchyma. For the neck, image noise was measured in soft-tissue equivalent areas at the level of the C4 cervical vertebrae. For the thorax anatomical region, image noise was measured in lung equivalent areas at the level of central part of the lung parenchyma, while for abdomen and pelvis anatomical region, image noise was measured in soft-tissue equivalent areas at the level of L4 lumbar vertebrae. At each anatomical region, image noise was measured for three consecutive image slices. Five ROIs were drawn throughout each image slice. The image noise was then derived from the average of the 15 measurements of the SD values. Quantitative image assessment and analysis was performed

Table 3 Routine 'adult' examination protocols

Anatomical region	Protocol acquisition parameters for routine CT examinations specified for adults			
	Head	Neck	Thorax	Abdomen & pelvis
Examination protocol	Head routine	Neck routine	Thorax routine	Abdomen routine
Parameter				
kV	120	120	120	120
Quality reference mAs	320	150	100	160
Beam width (mm)	16×0.75	16×1.5	16×1.5	16×1.5
Pitch	0.55	0.75	1.15	0.75
Rotation time (s)	1	0.75	0.5	0.5
Reconstruction kernel	H31s	B31s	B41f	B30f

The protocol acquisition parameters for each anatomical region in routine CT examination protocols specified for adults

Fig. 3 The scan boundaries of the four anatomical regions examined are shown on a whole body anteroposterior scout view of the 10-year-old phantom
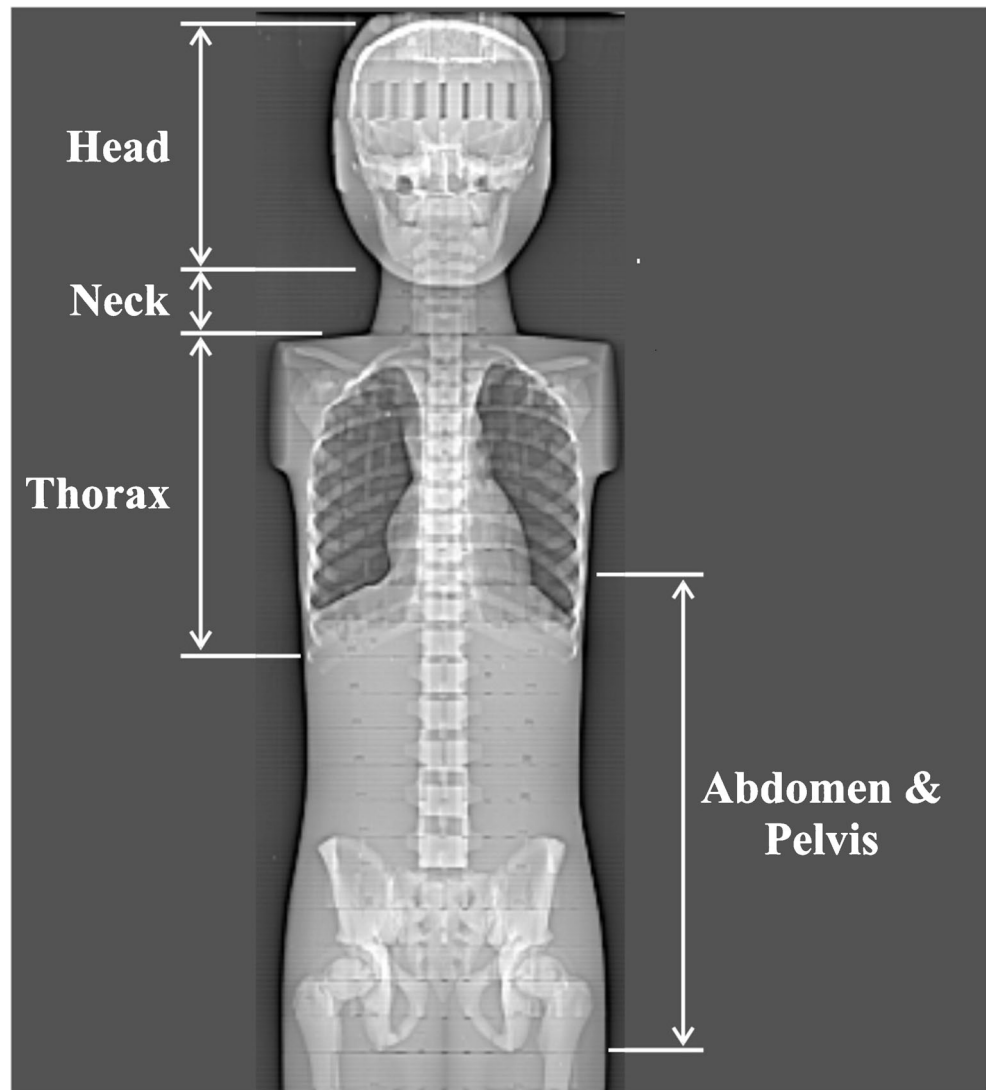
using the ImageJ image analysis software (version 1.46r, Java, NIH, USA). Modulated mAs and image noise comparison among phantoms for each acquisition was performed using the Student's t test for unpaired samples. A significant difference was set at a P value of less than 0.05. Statistical computations were performed using the MedCalc software package (MedCalc software, Belgium).

Results

Table 4 lists the phantoms' circumference (CIR) measured at specific anatomical sites, along with the corresponding mean modulated mAs_{mod} value, which was recorded upon the completion of each helical CT acquisition. Two mean mAs_{mod} values are tabulated for each CT acquisition. The first was

derived from acquisitions performed using the 'child' examination protocols, and the second was derived from acquisitions performed using 'adult' examination protocols. The mAs_{mod} values for head, neck and thorax are mostly lower in child compared to adult protocols, since mAs_{QR} settings are much lower in child than the corresponding setting for adult protocols. However, for abdomen/pelvis the mAs_{mod} values are higher in child protocols suggesting that ATCM might be less efficient in reducing radiation dose in children. As expected, mAs_{mod} values show an increase trend with CIR. This is more clearly illustrated for the abdomen/pelvis anatomical region, where mAs_{mod} was significantly increased from 45 for neonate to 142 for adult (III) when the 'child' abdomen routine examination protocol was selected ($P<0.05$). The corresponding increase for the 'adult' abdomen examination protocol was from 29 to 86 ($P<0.05$) The mAs_{mod} values listed in Table 4 were derived with the ATCM modulation strength setting set to the 'average decrease' for slim–'average

Table 4 Circumference (CIR) values measured at specific anatomic locations of head, neck, thorax, and abdomen and pelvis of each phantom along with the corresponding mAs_{mod} value derived from ATCM-activated CT acquisitions performed using examination protocols specified for children and adults

	Head		Neck		Thorax		Abdomen & pelvis	
	CIR (cm)	mAs_{mod} (Child/adult)	CIR (cm)	mAs_{mod} (Child/adult)	CIR (cm)	mAs_{mod} (Child/adult)	CIR (cm)	mAs_{mod} (Child/adult)
Neonate	34	61/74	18	43/59	40	31/32	32	45/29
1-year-old	46	72/125	21	37/54	57	28/26	42	51/26
5-year-old	48	75/134	26	38/51	56	30/28	54	59/31
10-year-old	51	79/143	29	49/66	61	33/27	58	69/34
10-year-old (I)	–	–	–	–	–	–	66	83/36
10-year-old (II)	–	–	–	–	–	–	76	94/45
Adult	57	90/159	41	55/67	95	77/63	80	107/59
Adult (I)	–	–	–	–	–	–	89	117/65
Adult (II)	–	–	–	–	–	–	98	132/76
Adult (III)	–	–	–	–	–	–	106	142/86

mAs_{mod} values refer to the mean modulated tube current–time product values averaged over the entire scan volume of each anatomical region

Modulation strength setting set to the default mode, i.e. 'average decrease' for slim–'average increase' for obese patients

increase' for obese patients. Moreover, as shown in Tables 2 and 4, the mAs_{QR}/mAs_{mod} value in thorax of the 10-year-old was 30/33, and in abdomen/pelvis of 5-year-old, 10-year-old, 10-year-old (I), and 10-year-old (II) was 55/59, 55/69, 55/83, and 55/94, respectively. This finding suggests that ATCM activation may potentially increase patient radiation dose in trunk CT examinations of children older than 5 years.

The effect of altering the modulation strength setting on the resulting mAs_{mod} values as a function of CIR is illustrated in Fig. 4 for 'child' (Fig. 4a) and 'adult' (Fig. 4b) abdomen routine examination protocols.

Figure 5 illustrates the $mAs_{mod}(z)$ profile curves derived from whole body CT acquisitions of the 5-year-old phantom (Fig. 5a) and the adult phantom (Fig. 5b) using the routine examination protocols for head, neck, thorax and abdomen anatomical regions specified for children and adults, respectively. Although all whole body CT scans were performed at the same mAs_{QR} setting (100), the $mAs_{mod}(z)$ profiles differ substantially among examination protocols.

Table 5 lists the image noise values obtained with fixed tube current acquisitions for each anatomical region and phantom. On average, image noise values were found to be lower for head and neck than for torso acquisitions. For the same anatomical region, the image was found to vary among phantoms. In particular, image noise varied from 1.5 to 5.3 HU for head, 1.9 to 7.8 HU for neck, 9.4 to 35.7 HU for thorax and 9.9 to 24.4 HU for abdomen/pelvis.

Table 6 lists the image noise values measured in the axial images along with the corresponding mAs_{mod} values for each phantom. For each anatomical region, two values are tabulated. These values were derived from CT acquisitions performed using examination protocols specified for children

and adults, respectively. Image noise was found to significantly increase from neonate to adult phantom ($P<0.05$). This increase was most pronounced in the abdomen and pelvis anatomical region of the phantoms.

Discussion

In this study we used ten anthropomorphic phantoms representing patients of varying age and body size to provide a detailed insight into how the CARE Dose 4D exposure modulation mechanism affects tube current and image noise. The results presented demonstrate quantitatively that mean modulated tube current and image noise are affected by (i) patient size, (ii) the patient target group for which the examination is prescribed ('child' versus 'adult'), (iii) anatomical region (head, thorax, etc.) and (iv) modulation strength setting (strong, average, weak).

Several studies have reported results on the efficiency of ATCM systems in delivering images of diagnostic quality at an optimized patient radiation dose [1–4, 15–22]. These studies have assessed the percentage dose reduction achieved when the ATCM is activated as $(mAs_{mod}−mAs_{QR})/mAs_{QR}$ %. Once the mAs_{QR} value is selected, the actual mAs is modulated online as the tube rotates around the patient and moves along the patient's long axis. If the attenuation caused by the examined patient is similar to that of a reference patient, the mAs_{mod} values are expected to be similar to the mAs_{QR}. The data presented in Tables 2, 3 and 4 suggest that the trunk of the reference 5-year-old patient considered by CARE Dose 4D closely matches the trunk of the ATOM phantom simulating the 5-year-old individual used here, but head and neck
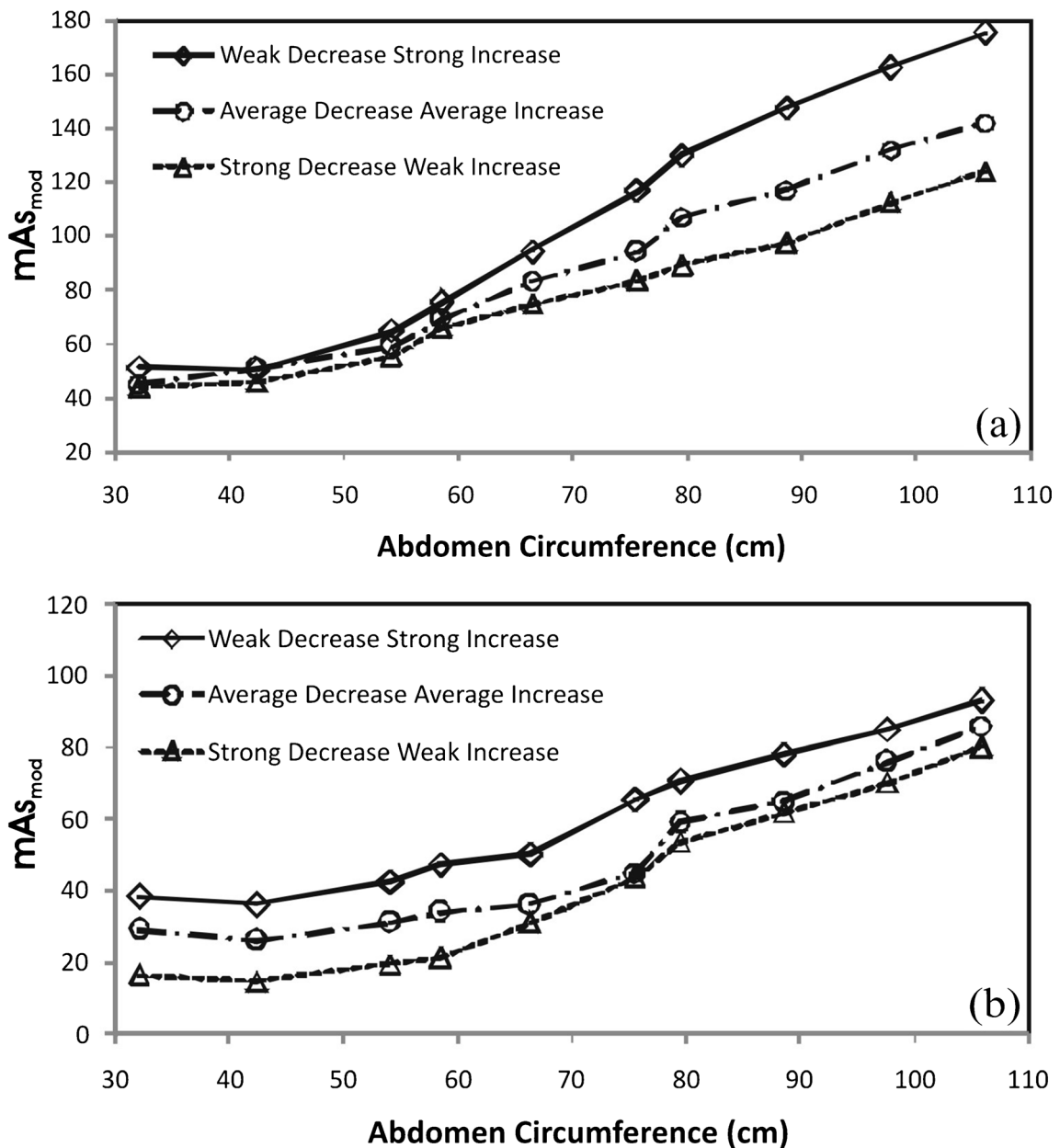
Fig. 4 mAs$_{mod}$ values as a function of the phantom's abdomen circumference at three different modulation strength settings for 'child' (**a**) and adult (**b**) abdomen routine examination protocol

regions do not. Indeed, the mAs$_{QR}$/mAs$_{mod}$ in the 5-year-old phantom was 30/30 for thorax and 55/59 for abdomen/pelvis, whereas it was 150/75 for head and 60/38 for neck. Besides, the data presented in Tables 2, 3 and 4 suggest that the size of the reference adult patient considered by CARE Dose 4D seems to be considerably larger than the Rando phantom simulating the average (height 1.73 m, weight 73.5 kg) adult individual. Indeed, the mAs$_{QR}$/mAs$_{mod}$ was 320/159 for head, 150/67 for neck, 100/63 for thorax and 160/59 for abdomen/pelvis. This finding is further illustrated in the Rando phantom simulating the adult (I), (II) and (III) individuals. Specifically, the mAs$_{QR}$/mAs$_{mod}$ for abdominal examinations was 160/65,

160/76 and 160/86 for adult (I), adult (II) and adult (III), respectively. Even the largest phantom considered here seems to be much smaller than the average adult considered by the system. These findings indicate the importance of using ATCM in adult examination protocols. Even for average size adult patients, the application of ATCM may result in considerable dose reduction compared to the stable mAs examination, in contrast to what might be a common conviction. Moreover, as shown in Table 4, the mean mAs$_{mod}$ value exceeded the mAs$_{QR}$ by 10 % (33 versus 30) in thorax of the 10-year-old, and by 71 % (55 versus 94) in abdomen/pelvis

Fig. 5 $mAs_{mod}(z)$ profiles derived from whole body ATCM-activated helical scans of the 5-year-old phantom (**a**) using the 'child' examination protocols specified for head, neck, thorax and abdomen anatomical regions (Table 2), and the adult phantom (**b**) using the corresponding 'adult' examination protocols (Table 3). All acquisitions were performed at the same mAs_{QR} setting (100) and with the modulation strength set to 'average' decrease for slim and average increase for obese patients
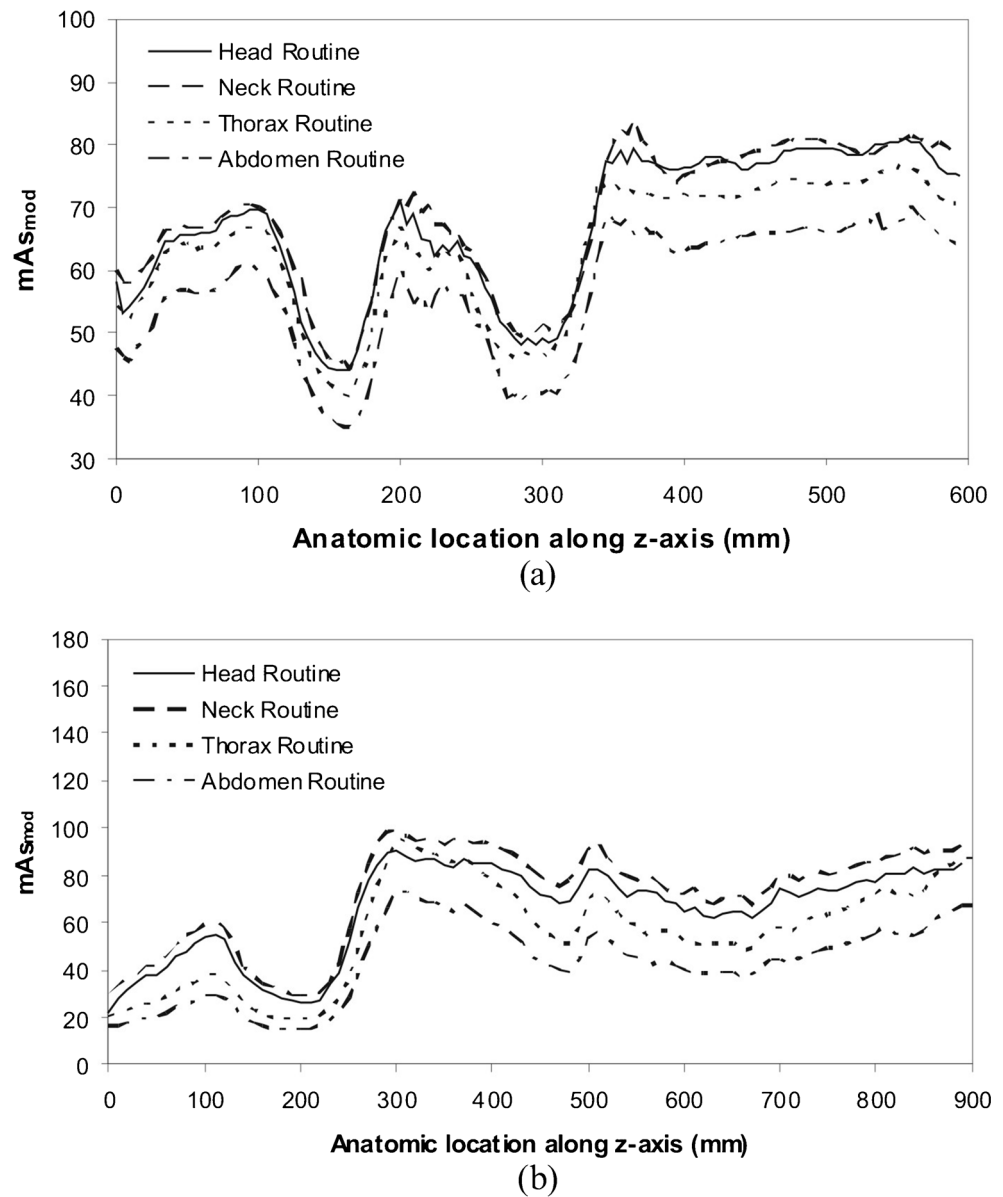

(a)

(b)

Table 5 Average image noise value obtained with fixed tube current acquisitions for each anatomical region and phantom

	Head		Neck		Thorax		Abdomen & pelvis	
	mAs_f	Image noise	mAs_f	Image noise	mAs_f	Image noise	mAs_f	Image noise
Neonate	90	4.7	40	7.8	17	30.3	30	18.6
1-year-old	150	4.6	40	7.6	17	35.7	30	24.4
5-year-old	220	2.5	60	5.7	20	26.1	30	31.5
10-year-old	320	1.5	60	5.8	30	12.6	55	10.8
Adult	320	5.3	150	1.9	100	9.4	160	9.9

Fixed tube current CT acquisitions were performed using the mAs_f values proposed by scanner's application guide on the basis of phantom's age for head and neck, and phantom's weight for torso examinations. Noise measurements were performed in axial image slices of 4 mm thickness. Image noise was measured at the level of central brain parenchyma for head, C2 cervical vertebrae for neck, central lung parenchyma for thorax and L4 lumbar vertebrae for abdomen and pelvis

Table 6 $mAs_{mod}(z)$ values obtained from the DICOM header of a selected axial image slice along with the corresponding average image noise value measured at that particular slice for each anatomical region and phantom, which was examined using a 'child' or 'adult' examination protocol

	Head		Neck		Thorax		Abdomen & pelvis	
	(Child/adult)		(Child/adult)		(Child/adult)		(Child/adult)	
	$mAs_{mod}(z)$	Image noise	$mAs_{mod}(z)$	Image noise	$mAs_{mod}(z)$	Image noise	$mAs_{mod}(z)$	Image noise
Neonate	62/100	3.7/2.5	54/72	4.6/3.3	17/27	9.6/7.9	40/20	6.2/7.4
1-year-old	77/137	3.6/2.9	51/78	4.7/3.6	14/26	11.8/8.9	47/23	7.5/8.4
5-year-old	82/146	3.9/3.4	62/86	5.4/3.5	21/28	11.6/10.0	62/26	8.6/10.8
10-year-old	83/147	4.2/3.7	53/88	5.3/3.9	17/29	12.2/9.3	72/30	8.5/11.3
10-year-old (I)							84/38	10.0/12.6
10-year-old (II)							101/50	12.4/13.8
Adult	80/146	4.0/3.6	54/96	5.7/4.1	37/48	12.3/10.8	90/47	12.6/14.5
Adult (I)							102/56	14.0/14.5
Adult (II)							136/77	16.4/18.9
Adult (III)							143/91	17.7/19.1

$mAs_{mod}(z)$ values were obtained from the DICOM header of the images used for image noise measurements. Noise measurements were performed in axial image slices of 4 mm thickness. Image noise was measured at the level of central brain parenchyma for head, C2 cervical vertebrae for neck, central lung parenchyma for thorax and L4 lumbar vertebrae for abdomen and pelvis

acquisition of 10-year-old (II) phantom. This finding suggests that in torso CT examinations of children older than 5 years, ATCM activation may increase radiation dose.

A comparison between image noise values obtained from fixed tube current (Table 5) with the corresponding values obtained from ATCM-activated acquisitions (Table 6) reveals that the default mAs_{QR} may be appropriately modified to generate images of similar noise to the corresponding images obtained from fixed tube current acquisitions. In particular, the mAs_f and noise values found in fixed tube current acquisitions in abdomen/pelvis of the adult phantom are 160 and 9.9 HU (Table 5). When the same acquisition is performed with the ATCM activated at mAs_{QR} 160, the mean modulated mAs_{mod} applied is 59 (63 % decrease) and the corresponding image noise 14.5 HU (Table 6). To achieve the same image noise (9.9 HU) between two acquisitions the mAs_{QR}/mAs_{mod} should be increased from 160/59 to 192/71 ($71 = 59 \times \sqrt{14.5}/\sqrt{9.9}$). Therefore, to achieve images of similar noise between fixed tube current and ATCM acquisitions the dose might be reduced by 56 %. Moreover, in the case of the abdomen/pelvis of the 10-year-old phantom the mAs_f and noise values found in fixed tube current acquisitions are 55 and 10.8 HU (Table 5). When the same acquisition is performed with the ATCM activated at mAs_{QR} 55, the mean modulated mAs_{mod} applied is 69 (25 % increase) and the corresponding image noise is 8.5 HU (Table 6). To achieve the same image noise (10.8 HU) between two acquisitions, the mAs_{QR}/mAs_{mod} should be decreased from 55/69 to 49/61 ($61 = 69 \times \sqrt{8.5}/\sqrt{10.8}$). Therefore, to achieve images of similar noise between fixed tube current and ATCM acquisitions the dose should be increased by 11 %.

Regarding ATCM-activated examinations, data shown in Table 6 indicate that resulting image noise is elevated as patient body size is increased. This is most clearly seen in the abdomen/pelvis anatomical region, where image noise increased in the adult (III) phantom compared to the average adult by 32 % and decreased in neonate compared to the average 5-year-old child by 28 %. This is consistent with the operation principle of the CARE Dose 4D system, which is designed to alter image noise relative to that obtained for the reference patient [6, 8]. This is based on the notion that different-sized patients require different levels of image noise to maintain diagnostic image quality. When imaging paediatric patients lower image noise, compared to adult patients, is preferred to improve delineation of anatomies of interest. Besides, higher noise levels may be tolerated when examining large-sized patients to avoid increased patient radiation dose.

Our data illustrate how the parameter ATCM 'modulation strength' affects the mean modulated tube current, and consequently the resulting image noise, in ATCM-activated examinations of different body regions. As shown in Fig. 4a for paediatric patients, (a) selecting 'strong' or 'weak decrease' instead of 'average decrease' the resulting mean modulated mAs values were found to be lower or higher, respectively, for patients with body size smaller than the average patient considered by the system and (b) selecting 'strong' or 'weak increase' instead of 'average increase' the resulting mean modulated mAs values were found to be higher or lower, respectively, for patients with body size larger than the average patient considered by the system. As shown in Fig. 4b for adult patients, selecting 'strong' or 'weak decrease' instead of 'average decrease' the resulting mean modulated mAs values

are lower or higher, respectively. This seems to be valid for the whole range of patient sizes studied here, since as discussed previously even the largest phantom employed seems to be smaller than 'the average adult individual' considered by the system. In other words, the selection of even the highest modulation strength setting may not be adequate to appropriately increase mean modulated mAs with respect to mAs_{QR} and deliver images of acceptable noise through the application of an appropriately high mAs_{mod} value.

Our findings indicate that the effect of ATCM on tube current and consequently image noise is dependent on the anatomical region for which a specific examination protocol is designed. This dependence is demonstrated in the $mAs_{mod}(z)$ profiles of Fig. 5. This means that, everything else being equal, a change of the selected examination protocol from thorax to abdomen results in a different ATCM behaviour. These findings may be useful in cases where the volume to be examined includes different anatomical regions. For example, data shown in Fig. 5 indicate that, in whole body trunk ATCM-activated CT examinations (thorax + abdomen/pelvis), lower mAs_{mod} values result when the abdomen/pelvis instead of the thorax protocol is selected. Specifically, when the thorax routine protocol is selected, the mAs_{mod}/noise values at the level of central lung parenchyma for thorax and L4 lumbar vertebrae for abdomen/pelvis are 80/3.8 HU and 62/8.3 HU, respectively (Fig. 5b). However, when the abdomen routine protocol is selected the corresponding mAs_{mod}/noise values are 62/6.5 HU and 47/14.5 HU, respectively (Fig. 5b). Although the thorax protocol produces images with less noise compared to the abdomen protocol, the latter is associated with less patient radiation dose and still provides thoracic images with less noise compared to those obtained when the thorax is examined alone (6.5 HU versus 10.8 HU) and abdominal images of similar noise to those obtained when abdomen/pelvis is examined alone (14.5 HU). Therefore, in whole body trunk ATCM-activated CT examinations, operators should select the abdomen/pelvis protocol rather than the thorax protocol to reduce patient radiation burden. This may be particularly useful in paediatric patients who are considered more radiosensitive than adults.

Clinical image quality was not evaluated in the current study. It should be noted that this study was performed using anthropomorphic phantoms. A further study on a large number of patients at various ages and body habitus is required to investigate the effect of ATCM on clinical image quality. Another limitation of this study is that it was limited to a single ATCM system, which was available in the CT suite installed in our institution. Other CT vendors adopt different concepts in defining the level of diagnostic image quality. It would be interesting to investigate the effect of other ATCM algorithms on radiation dose and image quality in patients of varying age and body size. Moreover, this study was conducted using a 16-row CT system. Modern wide area detector CT

systems are equipped with a higher number of detector rows, which feature longer z-axis coverage per tube rotation. There is evidence, however, that the CARE Dose 4D system investigated herein exhibits similar performance in CTs with a different detector configuration built by the same vendor [20].

In conclusion, this study demonstrates that ATCM can reduce patient radiation dose in adult individuals regardless of their body habitus. Overweight adult patients referred for CT imaging can benefit from ATCM activation, regarding the associated absorbed radiation dose, even when the highest available modulation strength setting is selected. On the contrary, ATCM may increase patient radiation dose in trunk CT examinations of children older than 5 years. Moreover, this study shows that whole body trunk ATCM-activated CT examinations should be performed with the abdomen/pelvis rather than the thorax protocol to reduce patient radiation burden. The detailed insight to the operation principles of the complex ATCM mechanism, provided here, may be exploited by CT operators to better understand how ATCM can be clinically implemented and maximize its benefits towards a more efficient radiation dose management in CT imaging.

References

1. Mulkens TH, Bellinck P, Baeyaert M, Ghysen D, Van Dijck X, Mussen E, Venstermans C, Termote J (2005) Use of an automatic exposure control mechanism for dose optimization in multi–detector row CT examinations: clinical evaluation. Radiology 237:213–223
2. Rizzo S, Kalra M, Schmidt B, Dalal T, Suess C, Flohr T, Blake M, Saini S (2006) Comparison of angular and combined automatic tube current modulation techniques with constant tube current CT of the abdomen and pelvis. Am J Roentgenol 186:673–679
3. Kalra M, Maher M, Toth T, Kamath R, Halpern E, Saini S (2004) Comparison of z-axis automatic tube current modulation technique with fixed tube current CT scanning of abdomen and pelvis. Radiology 232:347–353
4. Papadakis AE, Perisinakis K, Damilakis J (2008) Automatic exposure control in pediatric and adult multi-detector CT examinations: a phantom study on dose reduction and image quality. Med Phys 35: 4567–4576
5. Allen BC, Baker ME, Einstein DM, Remer EM, Herts BR, Achkar JP, Davros W, Novac E, Obuchowski N (2010) Effect of altering automatic exposure settings and image quality reference mAs on radiation dose, image quality, and diagnostic efficacy in MDCT enterography of active inflammatory Crohn's disease. Am J Roentgenol 195:89–100

6. McCollough C, Bruesewitz M, Kofler JM (2006) CT dose reduction and dose management tools: overview of available options. Radiographics 26:503–512

7. Kalra M, Maher M, Kamath R, Horiouchi T, Toth T, Halpern E, Saini S (2004) Sixteen-detector row CT of abdomen and pelvis: study for optimization of z-axis modulation technique performed in 153 patients. Radiology 233:241–249

8. Solomon JB, Li X, Samei E (2013) Relating noise to image quality indicators in CT examinations with tube current modulation. Am J Roentgenol 200:592–600

9. Kalra M, Brady T (2006) CARE Dose4D new technique for radiation dose reduction. Siemens Somatom Session 19:28–31

10. Bredenholler C, Feuerlein U (2006) Somatom sensation 16 application guide. Siemens Medical, Forchheim

11. Sookpeng S, Martin CJ, Gentle DJ, Lopez-Gonzalez MR (2014) Relationships between patient size, dose and image noise under automatic tube current modulation systems. J Radiol Prot 34:103–123

12. Söderberg M, Gunnarsson M (2010) The effect of different adaptation strengths on image quality and radiation dose using Siemens Care Dose 4D. Radiat Prot Dosim 139:173–179

13. Kalra M, Maher M, Toth T, Schmidt B, Westerman B, Morgan H, Saini S (2004) Techniques and applications of automatic tube current modulation for CT. Radiology 233:649–657

14. Kalender W, Wolf H, Suess C (1999) Dose reduction in CT by anatomically adapted tube current modulation. II. Phantom measurements. Med Phys 26:2248–2253

15. Papadakis AE, Perisinakis K, Oikonomou I, Damilakis J (2011) Automatic exposure control in pediatric and adult computed tomography examinations: can we estimate organ and effective dose from mean mAs reduction? Investig Radiol 46:654–662

16. Papadakis AE, Perisinakis K, Damilakis J (2007) Angular on-line tube current modulation in multidetector CT examinations of children and adults: the influence of different scanning parameters on dose reduction. Med Phys 34:2864–2874

17. Brisse H, Robilliard M, Savignoni A, Pierrat N, Gaboriaud G, De Rycke Y, Neuenschwander S, Aubert B, Rosenwald J (2009) Assessment of organ absorbed doses and estimation of effective doses from pediatric anthropomorphic phantom measurements for multi-detector row CT with and without automatic exposure control. Health Phys 97:303–314

18. van Straten M, Deak P, Shrimpton P, Kalender W (2009) The effect of angular and longitudinal tube current modulations on the estimation of organ and effective doses in x-ray computed tomography. Med Phys 36:4881–4889

19. Das M, Mahnken AH, Muhlenbruch G, Stargardt A, Weiss C, Sennst D, Flohr T, Gunther R, Wildberger J (2005) Individually adapted examination protocols for reduction of radiation exposure for 16-MDCT chest examinations. Am J Roentgenol 184:1437–1443

20. Tack D, De Maertelaer V, Gevenois P (2003) Dose reduction in multidetector CT using attenuation-based online tube current modulation. Am J Roentgenol 181:331–334

21. Greess H, Lutze J, Nomayr A, Wolf H, Horhorn T, Kalender W, Bautz W (2004) Dose reduction in subsecond multislice spiral CT examination of children by on-line tube current modulation. Eur Radiol 14:995–999

22. Papadakis AE, Perisinakis K, Raissaki M, Damilakis J (2013) Effect of x-ray tube parameters and iodine concentration on image quality and radiation dose in cerebral pediatric and adult CT angiography. Investig Radiol 48:192–199